Computers and Mathematics with Applications 125 (2022) 90–100

Contents lists available at ScienceDirect

Computers and Mathematics with Applications

www.elsevier.com/locate/camwa

Robust weak Galerkin finite element solvers for Stokes flow based on a lifting operator

Zhuoran Wang [a], Ruishu Wang [b,*], Jiangguo Liu [c]

[a] School of Mathematics (Zhuhai), Sun Yat-sen University, Zhuhai, Guangdong 519082, China
[b] School of Mathematics, Jilin University, Changchun, Jilin 130012, China
[c] Department of Mathematics, Colorado State University, Fort Collins, CO 80523, USA

ARTICLE INFO

Keywords:
Cuboidal hexahedra
Lifting operator
Local Arbogast-Correa/Tao spaces
Quadrilateral meshes
Stokes flow
Weak Galerkin

ABSTRACT

This paper presents novel finite element solvers for Stokes flow that are pressure-robust due to the use of a lifting operator. Specifically, weak Galerkin (WG) finite element schemes are developed for the Stokes problem on quadrilateral and hexahedral meshes. Local Arbogast-Correa or Arbogast-Tao spaces are utilized for construction of discrete weak gradients. The lifting operator lifts WG test functions into $H(\mathrm{div})$-subspaces and removes pressure dependence of velocity errors. The pressure robustness of these solvers is validated theoretically and illustrated numerically. Comparison with the non-robust classical Taylor-Hood (Q_2, Q_1) solver is presented.

1. Introduction

In this paper, we consider the following Stokes flow problem

$$\begin{cases} -\mu\Delta\mathbf{u} + \nabla p = \mathbf{f}, & \text{in } \Omega, \\ \nabla\cdot\mathbf{u} = 0, & \text{in } \Omega, \\ \mathbf{u} = \mathbf{g}, & \text{on } \partial\Omega, \end{cases} \tag{1}$$

where $\Omega \subset \mathbb{R}^d (d = 2, 3)$ is a bounded domain, $\mu > 0$ is the fluid kinematic viscosity, $\mathbf{u}$ is the unknown fluid velocity, p is the fluid pressure, $\mathbf{f}$ is a body force, and $\mathbf{g}$ is a boundary condition that satisfies the compatibility condition $\int_{\partial\Omega} \mathbf{g}\cdot\mathbf{n} = 0$ with $\mathbf{n}$ being the outward unit normal vector on the domain boundary $\partial\Omega$.

Among the numerical solvers for Stokes flow, the classical mixed finite element methods are popular choices [7]. Superconvergence has been investigated for the MINI elements [11]. In addition to the mixed finite element methods, a hybridizable discontinuous Galerkin (HDG) method was developed in [39]. More recent developments in HDG based on the M-decomposition can be found in [12]. A staggered discontinuous Galerkin method was developed in [49]. However, some popular classical finite element methods, e.g., Taylor-Hood elements [9,34] and the MINI element [5], are not robust [23], in the sense that the velocity error depends on the pressure. More specifically, when the velocity is approximated by polynomials of order k and the pressure is approximated by polynomials of order $k-1$, the velocity error may appear as

$$\|\nabla(\mathbf{u} - \mathbf{u}_h)\| \le C_1 h^k |\mathbf{u}|_{k+1} + C_2 \mu^{-1} h^k |p|_k, \tag{2}$$

where C_1, C_2 are positive constants (independent of μ). This clearly results in large velocity errors for small values of the viscosity parameter μ.

This issue is related to discretization of the body force term $(\mathbf{f}, \mathbf{v})$ in the variational formulation. Consider a Helmholtz decomposition $\mathbf{f} = \mathbf{w} + \nabla\phi$, where $\mathbf{w}$ is divergence-free and $\nabla\phi$ is irrotational. Assume the test function $\mathbf{v}$ is divergence-free and has a vanishing normal component on the domain boundary, then

$$(\mathbf{f}, \mathbf{v}) = (\mathbf{w}, \mathbf{v}) + (\nabla\phi, \mathbf{v}) = (\mathbf{w}, \mathbf{v}) - (\phi, \nabla\cdot\mathbf{v}) + \langle\phi, \mathbf{v}\cdot\mathbf{n}\rangle = (\mathbf{w}, \mathbf{v}). \tag{3}$$

As stated in [28,29], the velocity should not be affected by the additional irrotational force $\nabla\phi$, which should be balanced completely by the pressure gradient ∇p. However, in most cases, the test function is not divergence-free and a Helmholtz decomposition of $\mathbf{f}$ is difficult to obtain in numerical methods. One remedy is to replace discretization of $(\mathbf{f}, \mathbf{v})$ by that of $(\mathbf{f}, \pi_h\mathbf{v})$, where π_h is an appropriate reconstruction operator in the $H(\mathrm{div})$-sense.

Using divergence-free elements, e.g., the popular Scott-Vogelius elements [17,33], can overcome this issue, although it may require delicate mesh refinements or higher orders for interpolation. Another approach involves the grad-div stabilization [1,38], which may require delicate parameter tuning or additional equations.

* Corresponding author.
E-mail addresses: wangzhr25@mail.sysu.edu.cn (Z. Wang), wangrs_math@jlu.edu.cn (R. Wang), liu@math.colostate.edu (J. Liu).

https://doi.org/10.1016/j.camwa.2022.08.043
Received 17 April 2022; Received in revised form 27 July 2022; Accepted 24 August 2022

Pressure-robustness methods have also been developed to remove pressure dependence of velocity errors. Divergence-free elements were developed in [15,40,48]. Enriched divergence-free rational shape functions were used in [21,22]. Divergence-free schemes with tangential penalty were investigated in [13,43]. A divergence-free MAC scheme on triangular meshes was developed in [10]. Pressure-robust schemes using divergence-preserving velocity reconstruction were studied in [28,29]. Pressure-robust schemes based on the Taylor-Hood and MINI elements were developed in [25]. Continuous and discontinuous pressure elements were used in [8,23–26,47]. Virtual elements [14] are versatile and a pressure-robust virtual element method for Stokes flow was recently designed in [41].

The weak Galerkin (WG) finite element methods were developed in [43] for the second-order elliptic equation. Later in [36], the application of WG methods was extended to polygonal meshes with the help of stabilizers. One main idea of the WG methods is the usage of weak functions and weak derivatives. The shape functions are defined separately in element interiors and on inter-element boundaries. The differential operators are approximated in the weak sense at the element level. WG finite element methods have been developed for a wide range of problems, e.g., the elliptic problems [42,43], the Stokes problem [6,30,45], the linear elasticity problems [19,46], the Darcy equation [31], the div-curl systems [27], and the Cahn-Hilliard equation [44].

WG methodology was recently applied to development of pressure-robust Stokes solvers in [35,37]. The solvers in [35] apply to 2-dim problems and use more than necessary degrees of freedom in element interiors. The solvers in [37] need to go through decomposition of polytopals into simplexes.

In this paper, as motivated by the discussion around Equation (3) and the existing work, we develop robust Stokes solvers based on a lifting operator that lifts WG test functions into $H(\mathrm{div})$-subspaces, e.g., Arbogast-Correa or Arbogast-Tao spaces. These solvers are designed for quadrilateral and hexahedral meshes, which are equally flexible as simplicial meshes in accommodation of complicated domain geometry but use less elements, especially in 3-dim. For many applications, they align well with certain physical features of the problems to be solved. No stabilizer is needed in our schemes.

The rest of the paper is organized as follows. Section 2 develops local bases for Arbogast-Correa/Tao spaces. Section 3 introduces WG finite elements and a lifting operator that will play an important role later. Section 4 presents WG finite element methods (without and with use of the lifting operator). Section 5 presents rigorous analysis to show the solvers with the lifting operator are pressure-robust. The robustness is illustrated by numerical experiments in Section 6 including comparison with the classical Taylor-Hood solver for Stokes flow. The paper is concluded in Section 7 with remarks.

2. Local Arbogast-Correa and Arbogast-Tao spaces

Before getting into detailed discussion, we list some usual definitions and notations about function spaces and norms that are used in development of finite element methods. Let Ω be an open bounded domain in $\mathbb{R}^d$ $(d = 2, 3)$ with a Lipschitz continuous boundary. We adopt the standard definitions for Sobolev spaces $H^s(\Omega)$ (for $s \geq 0$) and the associated norms/seminorms. The seminorm $|\cdot|_{s,\Omega}$ is defined as

$$|v|_{s,\Omega} = \left(\sum_{|\alpha|=s} \int_{\Omega} |\partial^\alpha v|^2 \right)^{\frac{1}{2}}$$

with the notations for a multi-index and a partial derivative as shown below

$$\alpha = (\alpha_1, \alpha_2, ..., \alpha_d), \quad |\alpha| = \alpha_1 + \alpha_2 + ... + \alpha_d, \quad \partial^\alpha = \partial_{x_1}^{\alpha_1} \partial_{x_2}^{\alpha_2} ... \partial_{x_d}^{\alpha_d}.$$

The norm $\|\cdot\|_{s,\Omega}$ is defined as

$$\|v\|_{s,\Omega} = \left(\sum_{j=0}^{s} |v|_{j,\Omega}^2 \right)^{\frac{1}{2}}.$$

These definitions and notations can be extended to the closed bounded domain $\overline{\Omega}$ and individual elements in a finite element mesh as well.

The space $H^0(\Omega)$ coincides with $L^2(\Omega)$, the space of Lebesgue square-integrable functions. We denote by $(\cdot,\cdot)_\Omega$ the standard L^2-inner product on Ω and $\langle\cdot,\cdot\rangle_{\partial\Omega}$ the L^2-inner product on the boundary $\partial\Omega$. When there is no ambiguity, we omit the subscripts.

Finite element approximations start with domain discretization. While simplicial (triangular and tetrahedral) meshes are frequently used, quadrilateral and hexahedral meshes are equally versatile. As highlighted in [18], quadrilateral/hexahedral meshes are also flexible in accommodating complicated domain geometry but usually involve less unknowns in finite element schemes; these meshes could be set in good alignment with the geometric and physical features of many problems in real applications. In this paper, we focus on weak Galerkin finite element methods on quadrilateral and hexahedral meshes. Especially, we use convex quadrilaterals, and also cuboidal hexahedra, which are convex and have flat faces.

For a convex quadrilateral E, a bilinear mapping from the reference unit square $\hat{E} = [0,1]^2$ to E can be uniquely determined using the coordinates of the four vertices of E. Similarly, a trilinear mapping maps the reference unit cube $\hat{E} = [0,1]^3$ to a hexahedron [20].

Approximation of a scalar field on a quadrilateral or hexahedron utilizing the aforementioned bi/trilinear mapping is straightforward. But approximation of vector fields on quadrilaterals or hexahedra usually involves the Piola transformation.

Let $\hat{E}$ be the unit square/cube and E be a quadrilateral or hexahedron. The Piola transformation maps a vector field $\hat{\mathbf{u}}(\hat{\mathbf{x}})$ defined on $\hat{E}$ to a vector field $\mathbf{u}(\mathbf{x})$ defined on E via

$$\mathbf{u}(\mathbf{x}) = \mathcal{P}_E(\hat{\mathbf{u}}) = \frac{\mathbf{J}_E}{J_E}\, \hat{\mathbf{u}}(\hat{\mathbf{x}}), \tag{4}$$

where $\mathbf{x} = F_E(\hat{\mathbf{x}})$ is the previously mentioned bi/trilinear mapping, $\mathbf{J}_E$ is its Jacobian matrix and J_E is the Jacobian determinant. The Piola transformation preserves the normal fluxes and divergence [3] (p. 5 formulas (12)(13)).

The Arbogast-Correa and Arbogast-Tao mixed finite element pairs were introduced in [2,3], respectively. These elements use rational vector-valued shape functions due to the Piola transformation. They have advantages over the classical Raviart-Thomas elements, but global basis functions are hard to construct, especially for the 3-dim case (cuboidal hexahedra).

In this paper, we use the Arbogast-Correa/Tao (ACT) spaces in the weak Galerkin framework, but only local bases are needed.

Strictly speaking, there are three types of ACT spaces.

(i) *Local* space $ACT(E)$ on an individual quadrilateral or cuboidal hexahedron;
(ii) *Broken* space $\mathcal{ACT}(\mathcal{E}_h)$ on a quadrilateral or hexahedral mesh $\mathcal{E}_h$, which is simply the Cartesian product of all local ACT spaces;
(iii) *Global* space $ACT(\mathcal{E}_h)$ is understood as $\mathcal{ACT}(\mathcal{E}_h) \cap H(\mathrm{div}, \Omega)$, which implies normal continuity for the vector functions in $ACT(\mathcal{E}_h)$.

It is difficult, especially for hexahedra, to construct a global basis for $ACT(\mathcal{E}_h)$ in the mixed finite element context [3]. However, in the weak Galerkin framework, only the local ACT spaces are used, and certain global properties, e.g., normal continuity, can be reinforced through the bilinear forms used.

In this paper, we focus on the lowest-order local $AC_0(E)$ spaces in 2-dim and $AT_0(E)$ spaces in 3-dim. For convenience of presentation and also `deal.II` implementation, we introduce a unified notation

$$ACT_0(E) = \begin{cases} AC_0(E), & d = 2, \\ AT_0(E), & d = 3. \end{cases} \tag{5}$$

It is known [2,32] that $\dim(AC_0(E)) = 4$ and

$$AC_0(E) = P_0(E)^2 + \mathbf{x}\tilde{P}_0(E) + \mathcal{P}_E\mathbb{S}_0, \tag{6}$$

where $P_0(E)^2$ is the space of all constant vectors on E, $\tilde{P}_0(E)$ is the space of all homogeneous polynomials of degree 0, and $\mathbb{S}_0 = \text{Span}(\mathbf{s}_0)$ with $\mathbf{s}_0 = \begin{bmatrix} \hat{x} \\ -\hat{y} \end{bmatrix}$. Clearly, $\mathbb{S}_0$ is the space of divergence-free vector fields on the reference element $\hat{E} = [0,1]^2$. In other words, a local basis for $AC_0(E)$ can be chosen as [32]

$$\begin{bmatrix} 1 \\ 0 \end{bmatrix}, \begin{bmatrix} 0 \\ 1 \end{bmatrix}, \begin{bmatrix} X \\ Y \end{bmatrix}, \mathcal{P}_E \begin{bmatrix} \hat{x} \\ -\hat{y} \end{bmatrix}, \tag{7}$$

where $X = x - x_c$, $Y = y - y_c$ and (x_c, y_c) is the element center.

Similarly, $\dim(AT_0(E)) = 6$, and a local basis for $AT_0(E)$ can be chosen as

$$\begin{bmatrix} 1 \\ 0 \\ 0 \end{bmatrix}, \begin{bmatrix} 0 \\ 1 \\ 0 \end{bmatrix}, \begin{bmatrix} 0 \\ 0 \\ 1 \end{bmatrix}, \begin{bmatrix} X \\ Y \\ Z \end{bmatrix}, \mathcal{P}_E \begin{bmatrix} \hat{x} \\ -\hat{y} \\ 0 \end{bmatrix}, \mathcal{P}_E \begin{bmatrix} 0 \\ \hat{y} \\ -\hat{z} \end{bmatrix}, \tag{8}$$

where $X = x - x_c, Y = y - y_c, Z = z - z_c$ are the normalized coordinates with (x_c, y_c, z_c) being the element center, $(\hat{x}, \hat{y}, \hat{z})$ are the reference coordinates.

Lemma 1 *(ACT0 div and flux). An $ACT_0(E)$ space defined in (5) has the following properties.*

- *Divergence:*

$$\nabla \cdot \mathbf{u} \in P_0(E), \quad \forall \mathbf{u} \in ACT_0(E). \tag{9}$$

- *Normal flux: For any edge/face e of E,*

$$\mathbf{u} \cdot \mathbf{n} \in P_0(e), \quad \forall \mathbf{u} \in ACT_0(E). \tag{10}$$

See also [2,3,32]. □

Now we consider matrix-version local spaces $ACT_0(E)^d$. Specifically, $AC_0(E)^2$ is the space of 2×2 matrices whose row vectors are in $AC_0(E)$. So $\dim(AC_0(E)^2) = 8$. Similarly, $AT_0(E)^3$ is the space of 3×3 matrices whose row vectors are in $AT_0(E)$. Thus $\dim(AT_0(E)^3) = 18$.

3. Weak Galerkin FE elements and a lifting operator

The weak Galerkin finite element methodology differs from other existing finite element methods by considering shape functions separately defined in element interiors and inter-element boundaries (edges or faces). Discrete versions of differential operators (gradient, div, curl, etc.) are constructed via integration by parts for these shape functions. This brings a great deal of flexibility to approximation of the variables and their derivatives in many variational forms derived from partial differential equations. For convenience, we list briefly here the major WG notations used in this paper.

- E: A quadrilateral or hexahedra element, E° denotes its interior whereas E^∂ denotes its boundary;
- $\mathbf{v}_h = \{\mathbf{v}_h^\circ, \mathbf{v}_h^\partial\}$: A weak vector function; Such a WG shape function has two independent pieces: $\mathbf{v}_h^\circ$ is defined in E°, but $\mathbf{v}_h^\partial$ is defined on E^∂;
- $\nabla_w\mathbf{v}$: The weak gradient of a WG weak function $\mathbf{v}$, see definition in (11);
- $\nabla_w \cdot \mathbf{v}$: The weak divergence of a weak functions $\mathbf{v}$, see definition in (12);
- $\mathbf{\Lambda}_h$: The lifting operator defined in (14) that plays a critical role in ensuring pressure robustness;
- $\mathbf{\Pi}_h$: A global interpolation operator defined in (47) that facilitates the L^2 error analysis.

Now we consider WG finite elements $(P_0^d, P_0^d; ACT_0^d, P_0)$, where $d = 2, 3$ is the space dimension that should be clear from the context.

WG$(P_0^d, P_0^d; ACT_0^d, P_0)$ finite elements for quadrilateral and hexahedra. We consider WG(P_0^d, P_0^d) vector-valued discrete weak functions on E. On each element E, a vector-valued weak function $\mathbf{v} = \{\mathbf{v}^\circ, \mathbf{v}^\partial\}$ is defined in the element interior and element faces respectively.

The discrete weak gradients $\nabla_w\mathbf{v} \in ACT_0^d(E)$ is defined via integration by parts,

$$\int_E \nabla_w\mathbf{v} : W = \int_{E^\partial} \mathbf{v}^\partial \cdot (W\mathbf{n}) - \int_{E^\circ} \mathbf{v}^\circ \cdot (\nabla \cdot W), \quad \forall W \in ACT_0(E)^d, \tag{11}$$

where : is the colon product among matrices.

The discrete weak divergence $\nabla_w \cdot \mathbf{v} \in P_0(E)$ is calculated via integration by parts,

$$\int_E (\nabla_w \cdot \mathbf{v})w = \int_{E^\partial} \mathbf{v}^\partial \cdot (w\mathbf{n}) - \int_{E^\circ} \mathbf{v}^\circ \cdot (\nabla w), \quad \forall w \in P_0(E). \tag{12}$$

Note that we may take $w = 1$ in $P_0(E)$. But $\nabla w = \mathbf{0}$ in E°, the above formula is reduced to $\nabla_w \cdot \mathbf{v} = (\mathbf{v}^\partial \cdot \mathbf{n})|e|/|E|$.

Remarks. Note that $\mathbf{v}^\circ$ is defined in element interior E° and $\mathbf{v}^\partial$ is defined on element boundary E^∂. But for analysis later, we shall extend $\mathbf{v}^\circ$ to E^∂ and consider the discrepancy $\mathbf{v}^\partial - \mathbf{v}^\circ$, when needed.

Let $\mathcal{E}_h$ be a shape-regular convex quadrilateral or hexahedron partition of Ω. For any element $E \in \mathcal{E}_h$, let E° be its interior and E^∂ be its boundary. Denote by h_E its diameter. The mesh size of $\mathcal{E}_h$ is defined as $h = \max_{E\in\mathcal{E}_h} h_E$.

We consider the following finite element spaces

$$\begin{aligned} \mathbf{V}_h &= \{\mathbf{u}_h = \{\mathbf{u}_h^\circ, \mathbf{u}_h^\partial\} : \mathbf{u}_h^\circ|_{E^\circ} \in P_0(E^\circ)^d, \mathbf{u}_h^\partial|_e \in P_0(e)^d, \\ &\qquad \forall E \in \mathcal{E}_h, e \subset E^\partial\}, \\ W_h &= \{p \in L_0^2(\Omega) : p|_E \in P_0(E), \forall E \in \mathcal{E}_h\}. \end{aligned} \tag{13}$$

Note that for any $\mathbf{u}_h \in \mathbf{V}_h$, $\mathbf{u}_h^\partial$ is single-valued on each edge/face e. Let Γ_h be the set of all edges/faces on the domain boundary $\partial\Omega$. Denote by $\mathbf{V}_h^0$ the subspace of $\mathbf{V}_h$ with $\mathbf{u}_h^\partial|_{\Gamma_h} = \mathbf{0}$.

In general, an Arbogast-Correa or Arbogast-Tao space contains rational vector functions and is larger than the constant vector space, in which the WG shape functions reside. It will be beneficial to map or lift discrete weak vector shape functions into the space ACT_0, first elementwise and then mesh-wise.

Definition *(Lifting operator $\mathbf{\Lambda}_h$).* This operator maps from $\mathbf{V}_h$ to $ACT_0(\mathcal{E}_h)$, which is an $H(\text{div})$-subspace. For any $\mathbf{v} = \{\mathbf{v}^\circ, \mathbf{v}^\partial\} \in \mathbf{V}_h$,

$$\langle(\mathbf{\Lambda}_h\mathbf{v}) \cdot \mathbf{n}, w\rangle_e = \langle\mathbf{v}^\partial \cdot \mathbf{n}, w\rangle_e, \quad \forall w \in P_0(e), \forall e \subset E^\partial. \tag{14}$$

The definition implies that a lowest order vector-valued WG shape function has the same normal flux as its lifted image in $ACT_0(\mathcal{E}_h)$.

Remarks. The lifted image $\mathbf{\Lambda}_h\mathbf{v}$ is solely determined by the values of $\mathbf{v}^\partial$ on the inter-element boundaries. The interior part $\mathbf{v}^\circ$ makes no contribution.

We shall see later, with the help of the lifting operator $\mathbf{\Lambda}_h$, the weak Galerkin finite element solvers for Stokes problems are robust. More specifically, the numerical velocity errors are not affected by small values of the viscosity parameter μ.

4. WG finite element schemes for Stokes flow

For the Stokes boundary value problem (1), based on integration by parts, the variational formulation is established as follows. Seek $\mathbf{u} \in H^1(\Omega)^d$ and $p \in L_0^2(\Omega)$ such that $\mathbf{u}|_{\partial\Omega} = \mathbf{0}$ and

$$\begin{cases} \mu(\nabla \mathbf{u}, \nabla \mathbf{v}) - (p, \nabla \cdot \mathbf{v}) &= (\mathbf{f}, \mathbf{v}), \quad \forall \mathbf{v} \in H_0^1(\Omega)^d, \\ -(\nabla \cdot \mathbf{u}, q) &= 0, \quad \forall q \in L_0^2(\Omega), \end{cases} \tag{15}$$

where $L_0^2(\Omega)$ is the subspace of $L^2(\Omega)$ consisting of the functions that have mean-value zero, i.e., $\int_\Omega p\, d\mathbf{x} = 0$. The condition ensures uniqueness of the pressure solution and shall be inherited by finite element schemes.

One advantage of the weak Galerkin methodology is that the classical gradient or divergence in the variational form (15) can be replaced by the discrete weak gradient/divergence of WG shape functions and finite element schemes are readily established.

Scheme I. For Stokes boundary value problem (1), seek $\mathbf{u}_h \in \mathbf{V}_h$ and $p_h \in W_h$ such that $\mathbf{u}_h^\partial|_{\Gamma_h} = \mathbf{Q}_h^\partial \mathbf{g}$, and there hold

$$\begin{cases} \mathcal{A}_h(\mathbf{u}_h, \mathbf{v}) + \mathcal{B}_h(p_h, \mathbf{v}) &= \mathcal{F}_h(\mathbf{v}), \quad \forall \mathbf{v} \in \mathbf{V}_h^0, \\ \mathcal{B}_h(\mathbf{u}_h, q) &= 0, \quad \forall q \in W_h, \end{cases} \tag{16}$$

where

$$\begin{cases} \mathcal{A}_h(\mathbf{u}_h, \mathbf{v}) := \mu(\mathbf{u}_h, \mathbf{v})_{\mathcal{E}_h} := \mu \sum_{E \in \mathcal{E}_h} (\nabla_w \mathbf{u}_h, \nabla_w \mathbf{v})_E, \\ \mathcal{B}_h(p_h, \mathbf{v}) := -(p_h, \nabla_w \cdot \mathbf{v})_{\mathcal{E}_h} := -\sum_{E \in \mathcal{E}_h} (p_h, \nabla_w \cdot \mathbf{v})_E, \\ \mathcal{B}_h(\mathbf{u}_h, q) := -(\nabla_w \cdot \mathbf{u}_h, q)_{\mathcal{E}_h}, \\ \mathcal{F}_h(\mathbf{v}) := \sum_{E \in \mathcal{E}_h} (\mathbf{f}, \mathbf{v}^\circ)_E, \end{cases} \tag{17}$$

where $\mathbf{Q}_h^\partial$ is the L^2-projection operator from $L^2(e)^d$ to $P_0(e)^d$ on any edge/face e.

Note that our definition for $\mathcal{B}_h(\cdot,\cdot)$ may be slightly different than what is found in the literature. A negative sign is introduced in the 2nd equation in (16) to maintain symmetry of the discrete linear system.

Scheme II (based on the lifting operator). For Stokes boundary value problem (1), seek $\mathbf{u}_h \in \mathbf{V}_h$ and $p_h \in W_h$ such that $\mathbf{u}_h^\partial|_{\Gamma_h} = \mathbf{Q}_h^\partial \mathbf{g}$, and there holds

$$\begin{cases} \mathcal{A}_h(\mathbf{u}_h, \mathbf{v}) + \mathcal{B}_h(p_h, \mathbf{v}) &= \mathcal{F}_h^\Lambda(\mathbf{v}), \quad \forall \mathbf{v} \in \mathbf{V}_h^0, \\ \mathcal{B}_h(\mathbf{u}_h, q) &= 0, \quad \forall q \in W_h, \end{cases} \tag{18}$$

where $\mathcal{A}_h, \mathcal{B}_h$ are the same as in Scheme I. However,

$$\mathcal{F}_h^\Lambda(\mathbf{v}) = \sum_{E \in \mathcal{E}_h} (\mathbf{f}, \mathbf{\Lambda}_h \mathbf{v})_E. \tag{19}$$

The change in the linear form on the right-hand side of the 1st equation in (18) seems very little. But it brings in significant benefits that ensure robustness of the numerical scheme. We shall show theoretically and numerically that Scheme II is robust or locking-free, i.e., the convergence orders of the errors in velocity and pressure are well kept for small values of μ or large Reynolds numbers.

5. Analysis: robustness of scheme II

In this section, we show rigorously that Scheme II is robust.

5.1. Properties of the WG finite element spaces

First, we need to understand the properties of the WG finite element spaces.

Definition *(Local L^2-projections).* Three versions are considered: scalar, vector, and matrix.

- Q_h is the L^2-projection operator from $L^2(\Omega)$ onto space $P_0(\mathcal{E}_h)$.
- $\mathbf{Q}_h$: For each element $E \in \mathcal{E}_h$, $\mathbf{Q}_h^\circ$ is the L^2-projection operator from the space $L^2(E)^d$ to the space $P_0(E^\circ)^d$, whereas $\mathbf{Q}_h^\partial$ is the previously defined L^2-projection for element boundaries. On the whole mesh $\mathcal{E}_h$, $\mathbf{Q}_h = \{\mathbf{Q}_h^\circ, \mathbf{Q}_h^\partial\}$ is the L^2-projection from $L^2(\Omega)$ onto $\mathbf{V}_h$.
- $\mathcal{Q}_h$ is the L^2-projection from $L^2(\Omega)^{d\times d}$ onto space $ACT_0(\mathcal{E}_h)^d$.

WG commuting identities. Based on the definitions of discrete weak gradient and discrete weak divergence, the properties of ACT_0 spaces (9)-(10), and the definitions of the above projection operators, it is clear that, on each element $E \in \mathcal{E}_h$, for any $\mathbf{w} \in H^1(E)^d$, there hold

$$\begin{cases} (\nabla_w(\mathbf{Q}_h \mathbf{w}), W)_E = (\mathcal{Q}_h(\nabla \mathbf{w}), W)_E, \quad \forall W \in ACT_0(E)^d, \\ (\nabla_w \cdot (\mathbf{Q}_h \mathbf{w}), w)_E = (Q_h(\nabla \cdot \mathbf{w}), w)_E, \quad \forall w \in P_0(E). \end{cases} \tag{20}$$

These commuting identities will be frequently used later.

Definition *(Semi-norm on $\mathbf{V}_h$).* For $\mathbf{v} \in \mathbf{V}_h$, we define

$$|||\mathbf{v}|||^2 = \sum_{E \in \mathcal{E}_h} \|\nabla_w \mathbf{v}\|_E^2. \tag{21}$$

This is a semi-norm on $\mathbf{V}_h$, but it becomes a norm on $\mathbf{V}_h^0$.

Lemma 2 *(Trace inequalities). Consider any $E \in \mathcal{E}_h$. There exists a constant $C > 0$ such that for any $w \in H^1(E)$ and any edge/face $e \subset E^\partial$, we have*

$$\|w\|_e^2 \le C(h^{-1}\|w\|_E^2 + h\|\nabla w\|_E^2). \tag{22}$$

Moreover, for any $W \in ACT_0^d$, the following property holds true

$$\|W\|_E^2 \le Ch\|W\mathbf{n}\|_{E^\partial}^2. \tag{23}$$

A proof for the 2nd estimate needs the techniques used in [31] but is skipped here. □

Lemma 3 *(Bounding weak function discrepancy by its discrete weak gradient). For any $\mathbf{v} \in \mathbf{V}_h^0$, the following estimate holds*

$$\sum_{E \in \mathcal{E}_h} h^{-1}\|\mathbf{v}^\partial - \mathbf{v}^\circ\|_{E^\partial}^2 \le C|||\mathbf{v}|||^2, \tag{24}$$

where $C > 0$ is a constant independent of h and μ.

Proof. Let $\mathbf{v} \in \mathbf{V}_h^0$. Consider a fixed element $E \in \mathcal{E}_h$. There are $2d^2$ linear combination coefficients for the local space $ACT_0(E)^d$. But $\mathbf{v}^\partial$ offers $2d^2$ constant vectors on all edges/faces together. There exists a function $W \in ACT_0(E)^d$ such that

$$(W\mathbf{n})|_{E^\partial} = \mathbf{v}^\partial - \mathbf{v}^\circ.$$

Together with the definition of the discrete weak gradient, this implies (since $\nabla \mathbf{v}^\circ = 0$)

$$(\nabla_w \mathbf{v}, W)_E = (\nabla \mathbf{v}^\circ, W)_{E^\circ} + \langle \mathbf{v}^\partial - \mathbf{v}^\circ, W\mathbf{n}\rangle_{E^\partial} = \|\mathbf{v}^\partial - \mathbf{v}^\circ\|_{E^\partial}^2.$$

Applying the Cauchy-Schwarz inequality, Young's inequality, and the 2nd trace inequality in (23), (see [19] also), we obtain

$$\|\mathbf{v}^\partial - \mathbf{v}^\circ\|^2_{E^\partial} = (\nabla_w \mathbf{v}, W)_E \le \frac{\delta}{2}\|W\|^2_E + \frac{1}{2\delta}\|\nabla_w \mathbf{v}\|^2_E$$
$$\le \frac{\delta}{2} Ch \|W\mathbf{n}\|^2_{E^\partial} + \frac{1}{2\delta}\|\nabla_w \mathbf{v}\|^2_E.$$

Rearranging terms and then taking $\delta = 1/(Ch)$ yields

$$C^{-1}h^{-1}\|\mathbf{v}^\partial - \mathbf{v}^\circ\|^2_{E^\partial} \le \|\nabla_w \mathbf{v}\|^2_E,$$

which completes the proof. □

Remarks. In the estimate in the above lemma, the left-hand side can be understood as a derivative in the discrete sense (difference quotients), whereas the right-hand side involves the discrete weak gradient.

5.2. Properties of the lifting operator

The lifting operator $\mathbf{\Lambda}_h$ plays an important role. Replacing $(\mathbf{f}, \mathbf{v}^\circ)$ in Scheme I by $(\mathbf{f}, \mathbf{\Lambda}_h \mathbf{v})$, we obtain Scheme II.

Lemma 4. *The lifting operator $\mathbf{\Lambda}_h$ has the following property*

$$\sum_{E\in\mathcal{E}_h} \|\mathbf{\Lambda}_h \mathbf{v} - \mathbf{v}^\circ\|_E \le Ch|||\mathbf{v}|||, \qquad \forall \mathbf{v} = \{\mathbf{v}^\circ, \mathbf{v}^\partial\} \in \mathbf{V}_h. \tag{25}$$

Proof. Let $E \in \mathcal{E}_h$. By the definition of $\mathbf{\Lambda}_h$, we have

$$\langle (\mathbf{\Lambda}_h \mathbf{v} - \mathbf{v}^\circ)\cdot \mathbf{n}, w\rangle_{E^\partial} = \langle (\mathbf{v}^\partial - \mathbf{v}^\circ)\cdot \mathbf{n}, w\rangle_{E^\partial}, \quad \forall w \in P_0(E^\partial).$$

Setting $w = (\mathbf{\Lambda}_h \mathbf{v} - \mathbf{v}^\circ)\cdot \mathbf{n} \in P_0(E^\partial)$, we obtain

$$\|(\mathbf{\Lambda}_h \mathbf{v} - \mathbf{v}^\circ)\cdot \mathbf{n}\|^2_{E^\partial} = \langle (\mathbf{v}^\partial - \mathbf{v}^\circ)\cdot \mathbf{n}, (\mathbf{\Lambda}_h \mathbf{v} - \mathbf{v}^\circ)\cdot \mathbf{n}\rangle_{E^\partial}$$
$$\le \|\mathbf{v}^\partial - \mathbf{v}^\circ\|_{E^\partial} \|(\mathbf{\Lambda}_h \mathbf{v} - \mathbf{v}^\circ)\cdot \mathbf{n}\|_{E^\partial}.$$

A cancellation of $\|(\mathbf{\Lambda}_h \mathbf{v} - \mathbf{v}^\circ)\cdot \mathbf{n}\|_{E^\partial}$ yields

$$\|(\mathbf{\Lambda}_h \mathbf{v} - \mathbf{v}^\circ)\cdot \mathbf{n}\|_{E^\partial} \le \|\mathbf{v}^\partial - \mathbf{v}^\circ\|_{E^\partial}.$$

Applying the above inequality, (23), and the properties of $\mathbf{\Lambda}_h$, we obtain

$$\|\mathbf{\Lambda}_h \mathbf{v} - \mathbf{v}^\circ\|_E \le Ch^{\frac{1}{2}} \|(\mathbf{\Lambda}_h \mathbf{v} - \mathbf{v}^\circ)\cdot \mathbf{n}\|_{E^\partial} \le Ch(h^{-\frac{1}{2}}\|\mathbf{v}^\partial - \mathbf{v}^\circ\|_{E^\partial}).$$

A summation over the mesh yields the desired result. □

5.3. Error equations

Let $\mathbf{u} \in H^2(\Omega)^d$, $p \in H^1(\Omega)$ be the solutions of Stokes problem (1). Let $\mathbf{u}_h \in \mathbf{V}_h$, $p_h \in W_h$ be the numerical solutions of Scheme II. We split the errors as the projection errors and discrete errors as follows

$$\begin{cases} \mathbf{u} - \mathbf{u}_h = (\mathbf{u} - \mathbf{Q}_h \mathbf{u}) + \mathbf{e}_h, & \mathbf{e}_h := \mathbf{Q}_h \mathbf{u} - \mathbf{u}_h, \\ p - p_h = (p - Q_h p) + e_h, & e_h := Q_h p - p_h. \end{cases} \tag{26}$$

The projection errors $\mathbf{u} - \mathbf{Q}_h \mathbf{u}$, $p - Q_h p$ are determined by the approximation capacity of the finite element spaces. We focus on the discrete errors $\mathbf{e}_h$ and e_h.

Lemma 5 *(Scheme II truncation errors). Let $\mathbf{u} \in H^2(\Omega)^d$, $p \in H^1(\Omega)$ be the solutions of Stokes problem (1). Let $\mathbf{Q}_h \mathbf{u}$, $Q_h p$ be the L^2-projections defined previously. Then there hold*

$$\begin{cases} \mathcal{A}_h(\mathbf{Q}_h \mathbf{u}, \mathbf{v}) + \mathcal{B}_h(Q_h p, \mathbf{v}) = \mathcal{F}_h^\Lambda(\mathbf{v}) + \mu \mathcal{R}_1(\mathbf{v}) + \mu \mathcal{R}_2(\mathbf{v}), & \forall \mathbf{v} \in \mathbf{V}_h^0, \\ \mathcal{B}_h(\mathbf{Q}_h \mathbf{u}, q) = 0, & \forall q \in W_h, \end{cases} \tag{27}$$

where the remainders are

$$\begin{cases} \mathcal{R}_1(\mathbf{v}) = \sum_{E\in\mathcal{E}_h} \langle \mathbf{v}^\partial - \mathbf{v}^\circ, (Q_h \nabla \mathbf{u} - \nabla \mathbf{u})\mathbf{n}\rangle_{E^\partial}, \\ \mathcal{R}_2(\mathbf{v}) = \sum_{E\in\mathcal{E}_h} (\Delta \mathbf{u}, \mathbf{\Lambda}_h \mathbf{v} - \mathbf{v}^\circ)_E. \end{cases} \tag{28}$$

Proof. We perform a rigorous proof in five steps.

Step (i). To check $\mathcal{A}_h(\mathbf{Q}_h \mathbf{u}, \mathbf{v})$, we consider elementwise

$$\begin{aligned} (\nabla_w(\mathbf{Q}_h \mathbf{u}), \nabla_w \mathbf{v})_E &= (\mathcal{Q}_h(\nabla \mathbf{u}), \nabla_w \mathbf{v})_E && \text{(WG commuting identity)} \\ &= \langle \mathbf{v}^\partial, (\mathcal{Q}_h \nabla \mathbf{u})\mathbf{n}\rangle_{E^\partial} - (\mathbf{v}^\circ, \nabla\cdot(\mathcal{Q}_h \nabla \mathbf{u}))_{E^\circ} && \text{(Definition of } \nabla_w) \\ &= \langle \mathbf{v}^\partial, (\mathcal{Q}_h \nabla \mathbf{u})\mathbf{n}\rangle_{E^\partial} - \langle \mathbf{v}^\circ, (\mathcal{Q}_h \nabla \mathbf{u})\mathbf{n}\rangle_{E^\partial} && \text{(Integration by parts)} \\ &\quad + (\nabla \mathbf{v}^\circ, \mathcal{Q}_h \nabla \mathbf{u})_E && \text{(Note } \nabla \mathbf{v}^\circ = 0 \text{ zero matrix)} \\ &= \langle \mathbf{v}^\partial - \mathbf{v}^\circ, (\mathcal{Q}_h \nabla \mathbf{u})\mathbf{n}\rangle_{E^\partial}. \end{aligned} \tag{29}$$

Then summation over the whole mesh yields

$$\mathcal{A}_h(\mathbf{Q}_h \mathbf{u}, \mathbf{v}) = \mu \sum_{E\in\mathcal{E}_h} (\nabla_w(\mathbf{Q}_h \mathbf{u}), \nabla_w \mathbf{v})_E = \mu \sum_{E\in\mathcal{E}_h} \langle \mathbf{v}^\partial - \mathbf{v}^\circ, (\mathcal{Q}_h \nabla \mathbf{u})\mathbf{n}\rangle_{E^\partial}. \tag{30}$$

Step (ii). Recall the definition of $\mathcal{B}_h$ to get

$$\mathcal{B}_h(Q_h p, \mathbf{v}) = -\sum_{E\in\mathcal{E}_h} (Q_h p, \nabla_w \cdot \mathbf{v})_E. \tag{31}$$

Step (iii). To handle $\mathcal{F}_h^\Lambda(\mathbf{v})$, we use Stokes 1st equation $\mathbf{f} = -\mu\Delta \mathbf{u} + \nabla p$ to get

$$\begin{aligned} (\mathbf{f}, \mathbf{\Lambda}_h \mathbf{v})_E &= (-\mu\Delta \mathbf{u}, \mathbf{\Lambda}_h \mathbf{v})_E + (\nabla p, \mathbf{\Lambda}_h \mathbf{v})_E \\ &= -\mu(\Delta \mathbf{u}, \mathbf{\Lambda}_h \mathbf{v} - \mathbf{v}^\circ)_E - \mu(\Delta \mathbf{u}, \mathbf{v}^\circ)_E + (\nabla p, \mathbf{\Lambda}_h \mathbf{v})_E. \end{aligned} \tag{32}$$

For the 3rd term in the last line, we use integration by parts and the properties of Q_h and $\mathbf{\Lambda}_h$ to obtain

$$\begin{aligned} (\nabla p, \mathbf{\Lambda}_h \mathbf{v})_E &= \langle p, (\mathbf{\Lambda}_h \mathbf{v})\cdot \mathbf{n}\rangle_{E^\partial} - (p, \nabla\cdot(\mathbf{\Lambda}_h \mathbf{v}))_E \\ &= \langle p, (\mathbf{\Lambda}_h \mathbf{v})\cdot \mathbf{n}\rangle_{E^\partial} - (Q_h p, \nabla\cdot(\mathbf{\Lambda}_h \mathbf{v}))_E \\ &= \langle p, (\mathbf{\Lambda}_h \mathbf{v})\cdot \mathbf{n}\rangle_{E^\partial} - (Q_h p, \nabla_w \cdot \mathbf{v})_E. \end{aligned} \tag{33}$$

The facts that $\mathbf{v} \in \mathbf{V}_h^0$ and $\mathbf{\Lambda}_h \mathbf{v}$ has normal continuity together imply that

$$\sum_{E\in\mathcal{E}_h} (\nabla p, \mathbf{\Lambda}_h \mathbf{v})_E = -\sum_{E\in\mathcal{E}_h} (Q_h p, \nabla_w \cdot \mathbf{v})_E = \mathcal{B}_h(Q_h p, \mathbf{v}). \tag{34}$$

As for (32) 2nd line 2nd term, we have, due to integration by parts and $\nabla \mathbf{v}^\circ = 0$,

$$-(\Delta \mathbf{u}, \mathbf{v}^\circ)_E = -\langle \mathbf{v}^\circ, (\nabla \mathbf{u})\mathbf{n}\rangle_{E^\partial} + (\nabla \mathbf{v}^\circ, \nabla \mathbf{u})_E = -\langle \mathbf{v}^\circ, (\nabla \mathbf{u})\mathbf{n}\rangle_{E^\partial}. \tag{35}$$

Applying the normal continuity of $\nabla \mathbf{u}$ yields

$$-\mu \sum_{E\in\mathcal{E}_h} (\Delta \mathbf{u}, \mathbf{v}^\circ)_E = \mu \sum_{E\in\mathcal{E}_h} \langle \mathbf{v}^\partial - \mathbf{v}^\circ, (\nabla \mathbf{u})\mathbf{n}\rangle_{E^\partial}. \tag{36}$$

Combining (32), (34), (36) together gives

$$\mathcal{F}_h^\Lambda(\mathbf{v}) = -\mu \sum_{E\in\mathcal{E}_h} (\Delta \mathbf{u}, \Lambda_h \mathbf{v} - \mathbf{v}^\circ)_E + \mu \sum_{E\in\mathcal{E}_h} \langle \mathbf{v}^\partial - \mathbf{v}^\circ, (\nabla \mathbf{u})\mathbf{n}\rangle_{E^\partial} + \mathcal{B}_h(Q_h p, \mathbf{v}). \tag{37}$$

Step (iv). Now we combine the results in Steps (i)(ii)(iii) together to get

$$\begin{aligned} &\mathcal{A}_h(\mathbf{Q}_h \mathbf{u}, \mathbf{v}) + \mathcal{B}_h(Q_h p, \mathbf{v}) - \mathcal{F}_h^\Lambda(\mathbf{v}) \\ &= \mu \sum_{E\in\mathcal{E}_h} \langle \mathbf{v}^\partial - \mathbf{v}^\circ, (\mathcal{Q}_h \nabla \mathbf{u} - \nabla \mathbf{u})\mathbf{n}\rangle_{E^\partial} + \mu \sum_{E\in\mathcal{E}_h} (\Delta \mathbf{u}, \Lambda_h \mathbf{v} - \mathbf{v}^\circ)_E \\ &= \mu \mathcal{R}_1(\mathbf{v}) + \mu \mathcal{R}_2(\mathbf{v}), \end{aligned} \tag{38}$$

as appeared in the 1st of equation for the truncation errors (27).

Step (v). Since the exact velocity $\mathbf{u}$ satisfy $\nabla\cdot\mathbf{u}=0$, based on the 2nd WG commuting identity in (20), we have, for any $E\in\mathcal{E}_h$ and any $q\in P_0(E)$,

$$(\nabla_w\cdot(\mathbf{Q}_h\mathbf{u}),q)_E=(Q_h(\nabla\cdot\mathbf{u}),q)_E=0.$$

Hence $\mathcal{B}_h(\mathbf{Q}_h\mathbf{u},q)=0$ for any $q\in W_h$, as expected. □

Lemma 6 *(Scheme II error equations). There hold*

$$\begin{cases}\mathcal{A}_h(\mathbf{e}_h,\mathbf{v})+\mathcal{B}_h(e_h,\mathbf{v}) &= \mu\mathcal{R}_1(\mathbf{v})+\mu\mathcal{R}_2(\mathbf{v}), \quad \forall\mathbf{v}\in\mathbf{V}_h^0,\\ \mathcal{B}_h(\mathbf{e}_h,q) &= 0, \quad \forall q\in W_h,\end{cases}\tag{39}$$

where $\mathcal{R}_1,\mathcal{R}_2$ are already defined in (28).

Proof. Recall that the numerical solutions $\mathbf{u}_h$ and p_h satisfy the equations (18) in Scheme II, whereas the projections of the exact solutions satisfy the equations (27) derived in the previous lemma. Subtractions based on linearity of the linear and bilinear forms yield the desired equations in (39). □

5.4. Error estimates

Lemma 7 *(Inf-sup condition). There exists a constant $\beta>0$ independent of μ,h so that*

$$\sup_{\mathbf{v}\in\mathbf{V}_h^0,|||\mathbf{v}|||\neq0}\frac{|\mathcal{B}_h(\mathbf{v},q)|}{|||\mathbf{v}|||}\geq\beta\|q\|,\qquad\forall q\in W_h.\tag{40}$$

Proof. It is known that there exists a constant $C>0$ so that for any $q\in W_h\subset L_0^2(\Omega)$, there exists $\widetilde{\mathbf{v}}\in H_0^1(\Omega)^d$,

$$\frac{(\nabla\cdot\widetilde{\mathbf{v}},q)}{\|\nabla\widetilde{\mathbf{v}}\|}\geq C\|q\|.\tag{41}$$

Let $\mathbf{v}=\mathbf{Q}_h\widetilde{\mathbf{v}}\in\mathbf{V}_h$. The 1st WG commuting identity in (20) implies

$$|||\mathbf{v}|||^2=\sum_{E\in\mathcal{E}_h}\|\nabla_w\mathbf{v}\|_E^2=\sum_{E\in\mathcal{E}_h}\|\nabla_w\mathbf{Q}_h\widetilde{\mathbf{v}}\|_E^2=\sum_{E\in\mathcal{E}_h}\|\mathcal{Q}_h\nabla\widetilde{\mathbf{v}}\|_E^2\leq\|\nabla\widetilde{\mathbf{v}}\|^2.\tag{42}$$

Applying the 2nd WG commuting identity in (20), we obtain

$$\sum_{E\in\mathcal{E}_h}(\nabla_w\cdot\mathbf{v},q)_E=\sum_{E\in\mathcal{E}_h}(\nabla_w\cdot(\mathbf{Q}_h\widetilde{\mathbf{v}}),q)_E=\sum_{E\in\mathcal{E}_h}(Q_h\nabla\cdot\widetilde{\mathbf{v}},q)_E=\sum_{E\in\mathcal{E}_h}(\nabla\cdot\widetilde{\mathbf{v}},q)_E.$$

Therefore,

$$\frac{\sum_{E\in\mathcal{E}_h}(\nabla_w\cdot\mathbf{v},q)_E}{|||\mathbf{v}|||}\geq\frac{(\nabla\cdot\widetilde{\mathbf{v}},q)}{\|\nabla\widetilde{\mathbf{v}}\|}\geq C\|q\|,\tag{43}$$

as expected. □

Lemma 8 *(Scheme II truncation error estimates). Let $\mathbf{u}\in H^2(\Omega)^d$, $p\in H^1(\Omega)$ be the solutions of Stokes problem (1). Then for any $\mathbf{v}\in\mathbf{V}_h^0$, the remainders satisfy the following estimates*

$$\begin{aligned}&\mathcal{R}_1(\mathbf{v})\leq Ch\|\mathbf{u}\|_2|||\mathbf{v}|||,\\ &\mathcal{R}_2(\mathbf{v})\leq Ch\|\mathbf{u}\|_2|||\mathbf{v}|||,\end{aligned}\tag{44}$$

where $C>0$ is a constant independent of h and μ.

Proof. Using the Cauchy-Schwarz inequality, trace inequality (22), (24), and approximation properties of the projection operators, we obtain

$$\begin{aligned}\mathcal{R}_1(\mathbf{v}) &= \sum_{E\in\mathcal{E}_h}\langle\mathbf{v}^\partial-\mathbf{v}^\circ,(\mathcal{Q}_h\nabla\mathbf{u}-\nabla\mathbf{u})\mathbf{n}\rangle_{E^\partial}\\ &\leq C\left(\sum_{E\in\mathcal{E}_h}h^{-1}\|\mathbf{v}^\partial-\mathbf{v}^\circ\|_{E^\partial}^2\right)^{\frac12}\left(\sum_{E\in\mathcal{E}_h}h\|(\nabla\mathbf{u}-\mathcal{Q}_h\nabla\mathbf{u})\mathbf{n}\|_{E^\partial}^2\right)^{\frac12}\\ &\leq C|||\mathbf{v}|||\left(\sum_{E\in\mathcal{E}_h}\|\nabla\mathbf{u}-\mathcal{Q}_h\nabla\mathbf{u}\|_E^2+h^2|\nabla\mathbf{u}-\mathcal{Q}_h\nabla\mathbf{u}|_{1,E}^2\right)^{\frac12}\\ &\leq Ch\|\mathbf{u}\|_2|||\mathbf{v}|||.\end{aligned}$$

It follows from the Cauchy-Schwarz inequality and (25) that

$$\begin{aligned}\mathcal{R}_2(\mathbf{v}) &= \sum_{E\in\mathcal{E}_h}(\Delta\mathbf{u},\Lambda_h\mathbf{v}-\mathbf{v}^\circ)_E\\ &\leq C\left(\sum_{E\in\mathcal{E}_h}\|\Delta\mathbf{u}\|_E^2\right)^{\frac12}\left(\sum_{E\in\mathcal{E}_h}\|\Lambda_h\mathbf{v}-\mathbf{v}^\circ\|_E^2\right)^{\frac12}\\ &\leq Ch\|\mathbf{u}\|_2|||\mathbf{v}|||,\end{aligned}$$

as expected. □

Theorem 1 *(Estimates for discrete errors in velocity and pressure). Let $\mathbf{u}\in H^2(\Omega)^d$, $p\in H^1(\Omega)$ be the solutions of Stokes problem (1). Let $\mathbf{u}_h\in\mathbf{V}_h$, $p_h\in W_h$ be the numerical solution of Scheme II (lifting). Then the following estimates hold*

$$|||\mathbf{Q}_h\mathbf{u}-\mathbf{u}_h|||\leq Ch\|\mathbf{u}\|_2,\qquad\|Q_hp-p_h\|\leq C\mu h\|\mathbf{u}\|_2,\tag{45}$$

where $C>0$ is a constant independent of h and μ.

Proof. Taking $\mathbf{v}=\mathbf{e}_h$, $q=e_h$ in (39) and applying (44), we obtain

$$\mu|||\mathbf{e}_h|||^2=\mathcal{A}(\mathbf{e}_h,\mathbf{e}_h)=\mu\mathcal{R}_1(\mathbf{e}_h)+\mu\mathcal{R}_2(\mathbf{e}_h)\leq Ch\mu\|\mathbf{u}\|_2|||\mathbf{e}_h|||.$$

Then a cancellation yields

$$|||\mathbf{Q}_h\mathbf{u}-\mathbf{u}_h|||=|||\mathbf{e}_h|||\leq Ch\|\mathbf{u}\|_2.$$

A combination of the error equations, the inf-sup condition, and the estimates for the truncation errors (44) implies that

$$\begin{aligned}\beta\|e_h\| &\leq \sup_{\mathbf{v}\in\mathbf{V}_h^0,|||\mathbf{v}|||\neq0}\frac{|\mathcal{B}_h(\mathbf{v},e_h)|}{|||\mathbf{v}|||}\\ &= \sup_{\mathbf{v}\in\mathbf{V}_h^0,|||\mathbf{v}|||\neq0}\frac{\mathcal{A}_h(\mathbf{e}_h,\mathbf{v})-\mu\mathcal{R}_1(\mathbf{v})-\mu\mathcal{R}_2(\mathbf{v})}{|||\mathbf{v}|||}\\ &\leq C\mu h\|\mathbf{u}\|_2.\end{aligned}$$

This, in turn, yields

$$\|Q_hp-p_h\|=\|e_h\|\leq C\mu h\|\mathbf{u}\|_2,$$

as expected. □

Theorem 2 *(L^2-norm error estimates for pressure). Under the same conditions for Theorem 1, there holds*

$$\|p-p_h\|\leq Ch\|\mathbf{f}\|,\tag{46}$$

with $C>0$ being a constant that is independent of h and μ.

Proof. We have, by a triangle inequality,

$$\|p-p_h\|\leq\|p-Q_hp\|+\|Q_hp-p_h\|\leq Ch(\|p\|_1+\mu\|\mathbf{u}\|_2)\leq Ch\|\mathbf{f}\|,$$

where the condition for solution regularity $\mu\|\mathbf{u}\|_2+\|p\|_1\leq C\|\mathbf{f}\|$ has been used. □

To derive L^2-norm error estimates for velocity, we shall need a global interpolation operator.

Definition *(Global interpolation operator $\mathbf{\Pi}_h$).* This operator from $H^1(\Omega)^d$ to $ACT_0(\mathcal{E}_h)$ is defined as

$$\begin{cases} (\mathbf{\Pi}_h\mathbf{u})|_E = \mathbf{\Pi}_{h,E}(\mathbf{u}|_E), \\ \langle \mathbf{\Pi}_{h,E}\mathbf{u}\cdot\mathbf{n}, v\rangle_e = \langle \mathbf{u}\cdot\mathbf{n}, v\rangle_e, \quad \forall v\in P_0(e), \forall e\subset\partial E. \end{cases} \tag{47}$$

It has the following properties:

$$\begin{aligned} &(\nabla\cdot\mathbf{u}, v)_E = (\nabla\cdot\mathbf{\Pi}_{h,E}\mathbf{u}, v)_E, \quad \forall v\in P_0(E),\ \forall E\in\mathcal{E}_h, \\ &\|\mathbf{\Pi}_{h,E}\mathbf{u}-\mathbf{u}\| \le Ch\|\mathbf{u}\|_1, \\ &(\mathbf{u}-\mathbf{\Pi}_{h,E}\mathbf{u}, \mathbf{v})_E = 0, \quad \forall \mathbf{v}\in P_0(E)^d,\ \forall E\in\mathcal{E}_h. \end{aligned} \tag{48}$$

Now we introduce $\mathbf{\Pi}_h^d$ as a matrix interpolation operator, which acts on each row of the matrix, as defined by $\mathbf{\Pi}_h$. Then we have

$$\begin{aligned} (-\nabla\cdot W, \mathbf{v}^\circ) &= (-\nabla\cdot\mathbf{\Pi}_h^d W, \mathbf{v}^\circ) \quad \textit{(Applying (48) 1st eqn. on each row)} \\ &= \sum_{E\in\mathcal{E}_h} (\mathbf{\Pi}_{h,E}^d W, \nabla_w\mathbf{v})_E \qquad \textit{(Definition of } \nabla_w\textit{)} \\ &\quad - \sum_{E\in\mathcal{E}_h} \langle \mathbf{v}^\partial, (\mathbf{\Pi}_{h,E}^d W)\mathbf{n}\rangle_{E^\partial} \quad \textit{((}\Pi_{h,E}\nabla\Psi\textit{)}\mathbf{n}\textit{ continuity)} \\ &= (\mathbf{\Pi}_h^d W, \nabla_w\mathbf{v}). \end{aligned} \tag{49}$$

Remarks. The definitions of the operators $\mathbf{Q}_h$, $\mathbf{\Pi}_h$, and $\mathbf{\Lambda}_h$ together imply that for any $\mathbf{\Psi}\in H^1(\Omega)^d$, there holds

$$\langle \Lambda_h(\mathbf{Q}_h\mathbf{\Psi})\cdot\mathbf{n}, w\rangle_e = \langle (Q_h^\partial\mathbf{\Psi})\cdot\mathbf{n}, w\rangle_e = \langle \mathbf{\Psi}\cdot\mathbf{n}, w\rangle_e = \langle \mathbf{\Pi}_h\mathbf{\Psi}, w\rangle_e, \tag{50}$$

for any $w\in P_0(e)$ and any $e\subset E^\partial$. Therefore,

$$\mathbf{\Lambda}_h(\mathbf{Q}_h\mathbf{\Psi}) = \mathbf{\Pi}_h\mathbf{\Psi}. \tag{51}$$

Theorem 3 *(L^2-norm error estimates for velocity). Let $\mathbf{u}\in H^2(\Omega)^d$ be the exact solution of Stokes problem (1). Let $\mathbf{u}_h\in\mathbf{V}_h$ be the numerical solution of Scheme II (lifting). Assume $\mathbf{f}\in H^s(\Omega)^d$ with $0\le s\le 1$. Then*

$$\|\mathbf{Q}_h^\circ\mathbf{u}-\mathbf{u}_h^\circ\| \le Ch^{1+s}(\|\mathbf{f}\|_s + \|\mathbf{u}\|_2), \tag{52}$$

$$\|\mathbf{u}^\circ-\mathbf{u}_h^\circ\| \le Ch\|\mathbf{u}\|_2, \tag{53}$$

where $\mathbf{u}^\circ$ refers to the exact solution restricted to element interiors. For both cases, $C>0$ is a constant independent of h and μ.

Proof. We make a duality argument to estimate $\mathbf{e}_h^\circ = \mathbf{Q}_h^\circ\mathbf{u}-\mathbf{u}_h^\circ$. Assume that $\mathbf{\Psi}\in H^2(\Omega)^d$ and $\psi\in H^1(\Omega)\cap L_0^2(\Omega)$ are the solutions of the dual problem

$$\begin{cases} -\mu\Delta\mathbf{\Psi} + \nabla\psi &= \mathbf{e}_h^\circ, \quad \text{in } \Omega, \\ \nabla\cdot\mathbf{\Psi} &= 0, \quad \text{in } \Omega, \\ \mathbf{\Psi} &= \mathbf{0}, \quad \text{on } \partial\Omega. \end{cases} \tag{54}$$

Step (i). We test the 1st dual equation by $\mathbf{e}_h^\circ = \mathbf{Q}_h^\circ\mathbf{u}-\mathbf{u}_h^\circ$ to get

$$\|\mathbf{e}_h^\circ\|^2 = \sum_{E\in\mathcal{E}_h} (-\mu\Delta\mathbf{\Psi}, \mathbf{e}_h^\circ)_E + \sum_{E\in\mathcal{E}_h} (\nabla\psi, \mathbf{e}_h^\circ)_E. \tag{55}$$

Step (ii). Now we consider $\sum_{E\in\mathcal{E}_h} (\nabla\psi, \mathbf{e}_h^\circ)_E$. Here are some facts:

$$\psi\in L_0^2(\Omega), \quad Q_h\psi\in W_h, \quad \sum_{E\in\mathcal{E}_h} (Q_h\psi, \nabla_w\cdot\mathbf{e}_h)_E = \mathcal{B}_h(\mathbf{e}_h, Q_h\psi) = 0. \tag{56}$$

Applying integration by parts, the definitions of Q_h and $\nabla_w\cdot$, we obtain

$$\begin{aligned} (\nabla\psi, \mathbf{e}_h^\circ)_E &= \langle \psi\mathbf{n}, \mathbf{e}_h^\circ\rangle_{E^\partial} - (\psi, \nabla\cdot\mathbf{e}_h^\circ)_E \\ &= \langle \psi\mathbf{n}, \mathbf{e}_h^\circ\rangle_{E^\partial} - (Q_h\psi, \nabla\cdot\mathbf{e}_h^\circ)_E \\ &= \langle \psi\mathbf{n}, \mathbf{e}_h^\circ\rangle_{E^\partial} - \langle (Q_h\psi)\mathbf{n}, \mathbf{e}_h^\circ\rangle_{E^\partial} + (\nabla(Q_h\psi), \mathbf{e}_h^\circ)_E \\ &= \langle \psi\mathbf{n}, \mathbf{e}_h^\circ\rangle_{E^\partial} - \langle (Q_h\psi)\mathbf{n}, \mathbf{e}_h^\circ\rangle_{E^\partial} + \langle (Q_h\psi)\mathbf{n}, \mathbf{e}_h^\partial\rangle_{E^\partial} - (Q_h\psi, \nabla_w\cdot\mathbf{e}_h)_E. \end{aligned}$$

Summing over the mesh with application of the fact $\sum_{E\in\mathcal{E}_h} \langle \psi\mathbf{n}, \mathbf{e}_h^\partial\rangle_{E^\partial} = 0$ yields

$$\sum_{E\in\mathcal{E}_h} (\nabla\psi, \mathbf{e}_h^\circ)_E = \sum_{E\in\mathcal{E}_h} \langle (Q_h\psi-\psi)\mathbf{n}, \mathbf{e}_h^\partial - \mathbf{e}_h^\circ\rangle_{E^\partial}. \tag{57}$$

Applying the Cauchy-Schwarz inequality, the trace inequality (22), (24), the projection properties, and Theorem 1 leads to

$$\begin{aligned} \sum_{E\in\mathcal{E}_h} (\nabla\psi, \mathbf{e}_h^\circ)_E &= \sum_{E\in\mathcal{E}_h} \langle (Q_h\psi-\psi)\mathbf{n}, \mathbf{e}_h^\partial - \mathbf{e}_h^\circ\rangle_{E^\partial} \\ &\le \left(\sum_{E\in\mathcal{E}_h} h\|Q_h\psi-\psi\|_{E^\partial}^2\right)^{\frac12} \left(\sum_{E\in\mathcal{E}_h} h^{-1}\|\mathbf{e}_h^\partial - \mathbf{e}_h^\circ\|_{E^\partial}^2\right)^{\frac12} \\ &\le \left(\sum_{E\in\mathcal{E}_h} (\|Q_h\psi-\psi\|_E^2 + h^2\|\nabla(Q_h\psi-\psi)\|_E^2)\right)^{\frac12} |||\mathbf{e}_h||| \\ &\le Ch\|\psi\|_1|||\mathbf{e}_h||| \le Ch^2\|\psi\|_1\|\mathbf{u}\|_2. \end{aligned}$$

Step (iii). Applying (49) and the 1st WG commuting identity (20), we have

$$\begin{aligned} \sum_{E\in\mathcal{E}_h} (-\mu\Delta\mathbf{\Psi}, \mathbf{e}_h^\circ)_E &= \mu\sum_{E\in\mathcal{E}_h} (\mathbf{\Pi}_h^d(\nabla\mathbf{\Psi}), \nabla_w(\mathbf{Q}_h\mathbf{u}-\mathbf{u}_h))_E \\ &= \mu\sum_{E\in\mathcal{E}_h} (\mathbf{\Pi}_h^d(\nabla\mathbf{\Psi}) - \nabla\mathbf{\Psi}, \nabla\mathbf{u} - \nabla_w\mathbf{u}_h)_E \\ &\quad + \sum_{E\in\mathcal{E}_h} \mu(\nabla\mathbf{\Psi}, \nabla\mathbf{u} - \nabla_w\mathbf{u}_h)_E. \end{aligned} \tag{58}$$

Re-organizing the last term leads

$$\begin{aligned} \mu\sum_{E\in\mathcal{E}_h} (\nabla\mathbf{\Psi}, \nabla\mathbf{u} - \nabla_w\mathbf{u}_h)_E &= \mu\sum_{E\in\mathcal{E}_h} (\nabla\mathbf{\Psi}, \nabla\mathbf{u})_E \\ &\quad -\mu\sum_{E\in\mathcal{E}_h} (\nabla_w\mathbf{Q}_h\mathbf{\Psi}, \nabla_w\mathbf{u}_h)_E - \mu\sum_{E\in\mathcal{E}_h} (\nabla\mathbf{\Psi} - \nabla_w\mathbf{Q}_h\mathbf{\Psi}, \nabla_w\mathbf{u}_h)_E \\ &= \mu\sum_{E\in\mathcal{E}_h} (\nabla\mathbf{\Psi}, \nabla\mathbf{u})_E - \mu\sum_{E\in\mathcal{E}_h} (\nabla\mathbf{\Psi} - \mathcal{Q}_h\nabla\mathbf{\Psi}, \nabla_w\mathbf{u}_h - \nabla\mathbf{u})_E \\ &\quad -\mu\sum_{E\in\mathcal{E}_h} (\nabla_w\mathbf{Q}_h\mathbf{\Psi}, \nabla_w\mathbf{u}_h)_E - \mu\sum_{E\in\mathcal{E}_h} (\nabla\mathbf{\Psi} - \mathcal{Q}_h\nabla\mathbf{\Psi}, \nabla\mathbf{u} - \mathcal{Q}_h\nabla\mathbf{u})_E. \end{aligned}$$

Applying the Cauchy-Schwarz inequality, the projection properties, and Theorem 1, we obtain

$$\begin{aligned} &\mu\sum_{E\in\mathcal{E}_h} (\nabla\mathbf{\Psi} - \mathcal{Q}_h\nabla\mathbf{\Psi}, \nabla_w\mathbf{u}_h - \nabla\mathbf{u})_E \\ &= \mu\sum_{E\in\mathcal{E}_h} (\nabla\mathbf{\Psi} - \mathcal{Q}_h\nabla\mathbf{\Psi}, \nabla_w\mathbf{u}_h - \nabla_w(\mathbf{Q}_h\mathbf{u}))_E \\ &\quad +\mu\sum_{E\in\mathcal{E}_h} (\nabla\mathbf{\Psi} - \mathcal{Q}_h\nabla\mathbf{\Psi}, \mathcal{Q}_h(\nabla\mathbf{u}_h) - \nabla\mathbf{u})_E \\ &\le C\mu h\|\mathbf{\Psi}\|_2(|||\mathbf{e}_h||| + h\|\mathbf{u}\|_2) \le Ch^2\mu\|\mathbf{\Psi}\|_2\|\mathbf{u}\|_2. \end{aligned}$$

Applying the properties of matrix L^2-norm and the 2nd property of (48), we obtain

$$\mu\sum_{E\in\mathcal{E}_h} (\mathbf{\Pi}_h^d(\nabla\mathbf{\Psi}) - \nabla\mathbf{\Psi}, \nabla\mathbf{u} - \nabla_w\mathbf{u}_h)_E \le Ch^2\mu\|\mathbf{\Psi}\|_2\|\mathbf{u}\|_2. \tag{59}$$

Step (iv). It is easy to see that $\mathcal{B}_h(\mathbf{Q}_h\mathbf{\Psi}, p_h) = 0$. Combining the 1st equation of Scheme II, (51), and the 3rd property of operator $\mathbf{\Pi}_h$ (48), we obtain

$$\begin{aligned}\mu \sum_{E\in\mathcal{E}_h} (\nabla\mathbf{\Psi}, \nabla\mathbf{u})_E - \mu \sum_{E\in\mathcal{E}_h} (\nabla_w \mathbf{Q}_h\mathbf{\Psi}, \nabla_w \mathbf{u}_h)_E \\ = (\mathbf{f}, \mathbf{\Psi}) - (\mathbf{f}, \mathbf{\Lambda}_h(\mathbf{Q}_h\mathbf{\Psi})) = (\mathbf{f}, \mathbf{\Psi} - \mathbf{\Pi}_h\mathbf{\Psi}) \\ = (\mathbf{f} - \mathbf{Q}_h^\circ \mathbf{f}, \mathbf{\Psi} - \mathbf{\Pi}_h\mathbf{\Psi}) \le Ch^{1+s}\|\mathbf{f}\|_s \|\mathbf{\Psi}\|_2.\end{aligned} \tag{60}$$

Step (v). Combining the results in Steps (i)-(iv), we obtain

$$\begin{aligned}\|\mathbf{e}_h^\circ\|^2 = &\sum_{E\in\mathcal{E}_h} \langle (Q_h\psi - \psi)\mathbf{n}, \mathbf{e}_h^\partial - \mathbf{e}_h^\circ\rangle_{E^\partial} \\ &+\mu \sum_{E\in\mathcal{E}_h} (\mathbf{\Pi}_h^d(\nabla\mathbf{\Psi}) - \nabla\mathbf{\Psi}, \nabla\mathbf{u} - \nabla_w\mathbf{u}_h)_E \\ &+(\mathbf{f} - \mathbf{Q}_h^\circ\mathbf{f}, \mathbf{\Psi} - \mathbf{\Pi}_h\mathbf{\Psi}) \\ &-\mu \sum_{E\in\mathcal{E}_h} (\nabla\mathbf{\Psi} - \mathcal{Q}_h\nabla\mathbf{\Psi}, \nabla_w\mathbf{u}_h - \nabla\mathbf{u})_E \\ &-\mu \sum_{E\in\mathcal{E}_h} (\nabla\mathbf{\Psi} - \mathcal{Q}_h\nabla\mathbf{\Psi}, \nabla\mathbf{u} - \mathcal{Q}_h\nabla\mathbf{u})_E \\ \le Ch^{1+s}&(\|\mathbf{f}\|_s + \|\mathbf{u}\|_2)(\mu\|\mathbf{\Psi}\|_2 + \|\psi\|_1).\end{aligned} \tag{61}$$

Step (vi). Combining the estimates above and the dual solution regularity condition

$$\mu\|\mathbf{\Psi}\|_2 + \|\psi\|_1 \le C\|\mathbf{e}_h^\circ\| \tag{62}$$

gives

$$\|\mathbf{e}_h^\circ\| \le Ch^{1+s}(\|\mathbf{f}\|_s + \|\mathbf{u}\|_2),$$

as desired. Then, by the projection properties and a triangle inequality,

$$\begin{aligned}\|\mathbf{u}^\circ - \mathbf{u}_h^\circ\| &\le \|\mathbf{u}^\circ - \mathbf{Q}_h^\circ\mathbf{u}\| + \|\mathbf{Q}_h^\circ\mathbf{u} - \mathbf{u}_h^\circ\| \\ &\le Ch\|\mathbf{u}\|_2 + Ch^{1+s}(\|\mathbf{f}\|_s + \|\mathbf{u}\|_2) \le Ch(\|\mathbf{f}\|_s + \|\mathbf{u}\|_2),\end{aligned} \tag{63}$$

as claimed in the Theorem. □

5.5. Reasons why Scheme II works but Scheme I does not

Now we examine why Scheme I does not work. Notice that we have the same projections $\mathbf{Q}_h\mathbf{u}$, Q_hp from the exact solutions. Plugging them into Scheme I, we obtain truncation errors as below

$$\begin{cases}\mathcal{A}_h(\mathbf{Q}_h\mathbf{u}, \mathbf{v}) + \mathcal{B}_h(Q_hp, \mathbf{v}) = \mathcal{F}_h(\mathbf{v}) + \mu\mathcal{R}_1(\mathbf{v}) + \widetilde{\mathcal{R}}_1(\mathbf{v}), \\ \mathcal{B}_h(\mathbf{Q}_h\mathbf{u}, q) = 0,\end{cases} \tag{64}$$

where the bilinear forms $\mathcal{A}_h, \mathcal{B}_h$ are the same for Schemes I & II, the linear form $\mathcal{F}_h = \sum_{E\in\mathcal{E}_h}(\mathbf{f}, \mathbf{v}^\circ)_E$ (with no lifting) is defined in (17). Moreover, the truncation error $\mathcal{R}_1$ is the same as that in Lemma 5 Equation (28). But the other truncation error term takes the following form.

$$\widetilde{\mathcal{R}}_1(\mathbf{v}) = \sum_{E\in\mathcal{E}_h} \langle \mathbf{v}^\circ - \mathbf{v}^\partial, (Q_hp - p)\mathbf{n}\rangle_{E^\partial}. \tag{65}$$

Setting $\mathbf{v} = \mathbf{Q}_h\mathbf{u} - \mathbf{u}_h$, we obtain an error estimate for Scheme I:

$$\mu\|\nabla_w(\mathbf{Q}_h\mathbf{u} - \mathbf{u}_h)\| \le C\mu h\|\mathbf{u}\|_2 + Ch\|p\|_1. \tag{66}$$

For Scheme II (with lifting), there holds

$$\mu\|\nabla_w(\mathbf{Q}_h\mathbf{u} - \mathbf{u}_h)\| \le C\mu h\|\mathbf{u}\|_2.$$

So Scheme II velocity error does NOT depend on pressure but Scheme I does. The lifting operator plays a critical role for pressure robustness of Scheme II.

6. Numerical experiments

This section presents numerical experiments on the new solvers in this paper and also existing solvers, e.g., the classical Taylor-Hood methods. It will be demonstrated that the Taylor-Hood solvers are not robust but the new WG solvers (in Scheme II) are indeed robust. The numerical procedures for these two schemes are similar to many other continuous or weak Galerkin finite element methods: from mesh generation to computation of element stiffness matrices, and their assembly. However, it is interesting to notice the difference between the sparsity patterns of Scheme I and Scheme II as follows

$$\begin{cases}\text{Scheme I: } \begin{bmatrix}\mathcal{A}_h(\cdot,\cdot) & \mathcal{A}_h(\cdot,\cdot) & \\ \mathcal{A}_h(\cdot,\cdot) & \mathcal{A}_h(\cdot,\cdot) & \mathcal{B}_h(\cdot,\cdot) \\ & \mathcal{B}_h(\cdot,\cdot) & \end{bmatrix}\begin{bmatrix}\mathbf{u}^\circ \\ \mathbf{u}_h^\partial \\ p_h\end{bmatrix} = \begin{bmatrix}(\mathbf{f}, \mathbf{v}^\circ) \\ \mathbf{0} \\ \mathbf{0}\end{bmatrix}, \\ \text{Scheme II: } \begin{bmatrix}\mathcal{A}_h(\cdot,\cdot) & \mathcal{A}_h(\cdot,\cdot) & \\ \mathcal{A}_h(\cdot,\cdot) & \mathcal{A}_h(\cdot,\cdot) & \mathcal{B}_h(\cdot,\cdot) \\ & \mathcal{B}_h(\cdot,\cdot) & \end{bmatrix}\begin{bmatrix}\mathbf{u}_h^\circ \\ \mathbf{u}_h^\partial \\ p_h\end{bmatrix} = \begin{bmatrix}\mathbf{0} \\ (\mathbf{f}, \mathbf{\Lambda}_h\mathbf{v}^\partial) \\ \mathbf{0}\end{bmatrix}.\end{cases} \tag{67}$$

Scheme II shows a better matching of sparsity of the stiffness matrix and RHS.

Example 1 *(A 2-dim example with known analytical solutions)*. Here we consider the domain $\Omega = (0,1)^2$, the exact solutions are

$$\mathbf{u} = \begin{bmatrix}\sin(\pi x) \\ -\pi y\cos(\pi x)\end{bmatrix}, \qquad p = \sin(\pi x)\cos(\pi y). \tag{68}$$

Nonhomogeneous Dirichlet boundary conditions are posed on the domain boundary using the values of the exact solution for velocity. Clearly, the velocity and pressure solutions are infinitely smooth and the pressure has mean value zero. The problem is solved by WG Schemes I & II with different μ values on trapezoidal meshes (with slant parameter 0.25) that have been used in [4,32].

Shown in Table 1 are the results of Scheme I. For $\mu = 1$, the errors in velocity and pressure exhibit 1st order convergence. But for $\mu = 10^{-6}$, the errors in velocity are simply too large, although there may be some kind of convergence (even super-convergence). Scheme I is not robust.

Shown in Table 2 are the results of Scheme II. For $\mu = 1, 10^{-6}$ or other small values (not tabulated here), the errors in velocity and pressure exhibit always 1st order convergence. It is also observed that the divergence residual $\sum_{E\in\mathcal{E}_h}(\nabla_w\cdot\mathbf{u}_h)|E|$ are fluctuating at the level of machine zero. Scheme II is indeed robust.

Example 2 *(Flow through a bent duct)*. This example is adopted from [16]. The duct itself has diameter a. The bent part has a semi-circle shape with an inner diameter b. The duct has a straight piece of length l in both upper and lower parts. When Cartesian coordinates are used for domain geometry, the entry is described as $\{(x,y) : x = 0, a+b \le y \le 2a+b\}$, the exit is described as $\{(x,y) : x = 0, 0 \le y \le a\}$. Gravity $\mathbf{f} = [0, -\rho g]^T$ is considered, where ρ is fluid density and g is the gravitational constant. A Poiseuille profile of inflow is prescribed at the entry as

$$\mathbf{u}_D(x,y) = \begin{bmatrix}(y-(a+b))((2a+b)-y) \\ 0\end{bmatrix}, \quad \text{for } x = 0, y \in [a+b, 2a+b]. \tag{69}$$

Dirichlet $\mathbf{u}_D = \mathbf{0}$ (no-slip) boundary condition is specified on the peripheral.

Naturally, quadrilateral meshes are used for domain discretization. Schemes I and II (with lifting) are applied. Various values of μ have

Table 1
Example 1: Results by (non-robust) Scheme I on trapezoidal meshes.

$1/h$	$\|u-u_h^\circ\|$	Rate	$\|p-p_h\|$	Rate	$\|u-u_h^\circ\|$	Rate	$\|p-p_h\|$	Rate
	$\mu=1$				$\mu=10^{-6}$			
8	1.8439E-1	–	1.2769E-1	–	3.2736E+3	–	8.4716E-2	–
16	9.2409E-2	0.99	6.2157E-2	1.03	8.6406E+2	Errors	4.1713E-2	1.02
32	4.6231E-2	0.99	3.0957E-2	1.00	2.1989E+2	are	2.0690E-2	1.01
64	2.3119E-2	0.99	1.5490E-2	0.99	5.5291E+1	too	1.0310E-2	1.00
128	1.1559E-2	0.99	7.7537E-3	0.99	1.3848E+1	large	5.1488E-3	1.00

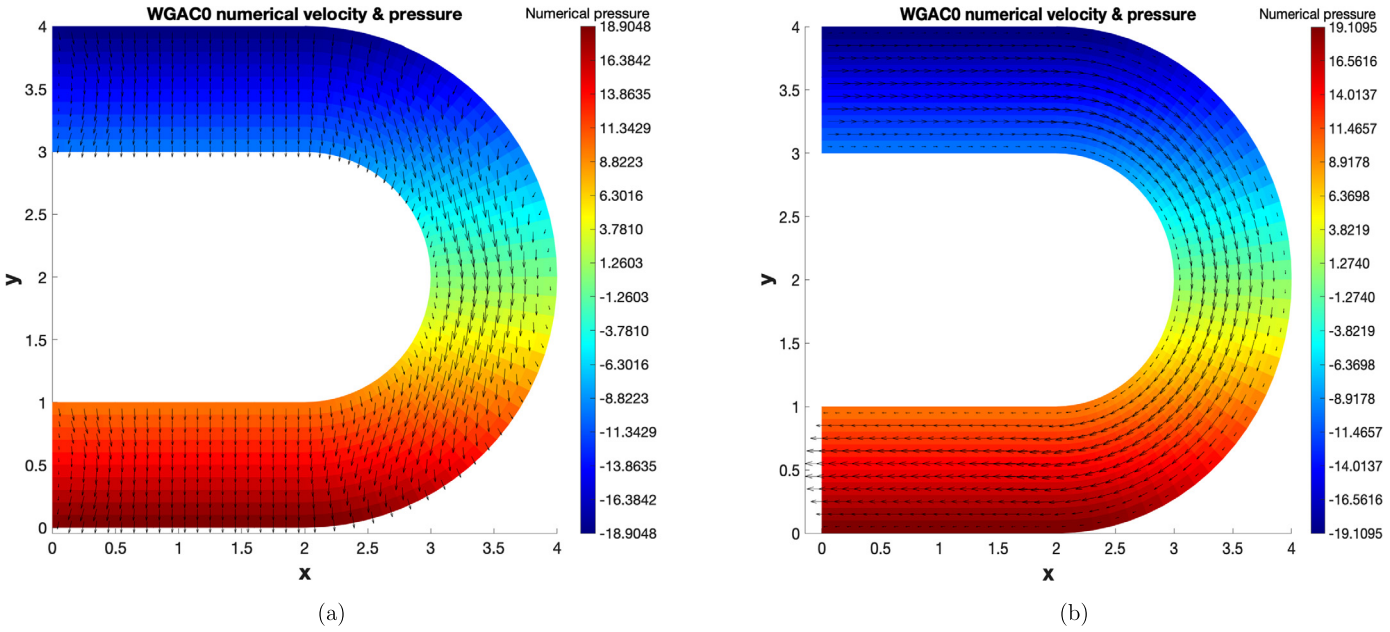

Fig. 1. Example 2: Stokes flow (gravity considered) in a bent duct ($\mu = 10^{-4}$). (a) Spurious velocity produced by Scheme I; (b) Numerical velocity and pressure produced by Scheme II (with lifting).

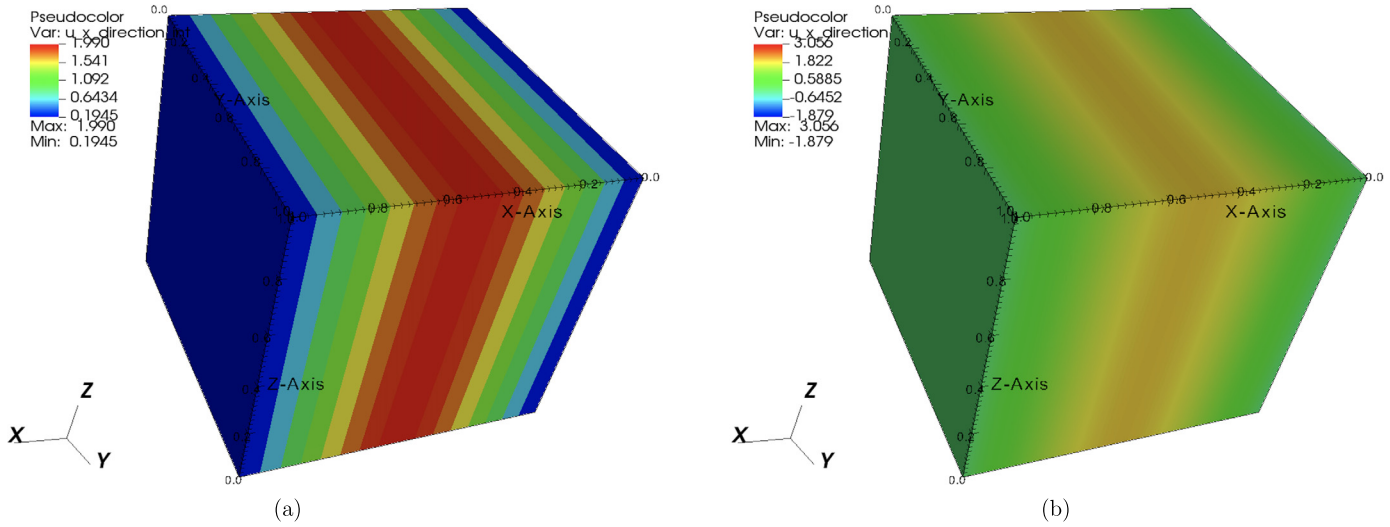

Fig. 2. Example 3 ($\mu = 10^{-6}, h = 1/16$): Comparison of numerical velocity 1st component. (a) WG Scheme II; (b) Taylor-Hood (Q_2, Q_1). The results by the latter are un-reliable.

been tested in numerical experiments. While results look good for both schemes when $\mu = 1$ (not reported though), the results of Scheme I become spurious when μ gets smaller.

Shown in Fig. 1 are numerical results with $a = 1, b = 2, l = 2$, $\rho = 1$, and $\mu = 10^{-4}$. Clearly, the velocity results in Panel (a) by Scheme I are non-physical, whereas the results in Panel (b) by Scheme II are reasonable.

Example 3 *(A 3-dim problem).* This example is taken from `deal.II` tutorial *step-56*. The exact solutions for velocity and pressure are

$$\mathbf{u} = \begin{bmatrix} 2\sin(\pi x) \\ -\pi y \cos(\pi x) \\ -\pi z \cos(\pi x) \end{bmatrix}, \qquad p = \sin(\pi x)\cos(\pi y)\sin(\pi z). \tag{70}$$

Table 2
Example 1: Results by (robust) Scheme II on trapezoidal meshes.

$1/h$	$\|u-u_h^\circ\|$	Rate	$\|p-p_h\|$	Rate	Div residual
$\mu=1$					
8	1.8539E-1	–	2.3126E-1	–	-2.1510E-16
16	9.2560E-2	1.00	8.8250E-2	1.38	−9.5409E-17
32	4.6251E-2	1.00	3.5782E-2	1.30	−2.0599E-16
64	2.3121E-2	1.00	1.6003E-2	1.16	−1.1709E-17
128	1.1560E-2	1.00	7.6550E-3	1.06	−9.9312E-17
$\mu=10^{-6}$					
8	1.8539E-1	–	8.1673E-2	–	-1.0408E-16
16	9.2560E-2	1.00	4.1032E-2	0.99	5.3776E-17
32	4.6251E-2	1.00	2.0540E-2	0.99	−2.1076E-16
64	2.3121E-2	1.00	1.0273E-2	0.99	−1.2143E-17
128	1.1560E-2	1.00	5.1370E-3	0.99	−6.1392E-17

Table 3
Example 3: Results by WG Scheme II on cubic meshes.

$1/h$	$\|u-u_h^\circ\|$	Rate	$\|p-p_h\|$	Rate	$\|\|\|Q_h^\circ u-u_h^\circ\|\|\|$	Rate
$\mu=1$						
8	2.8384E-1	–	3.2127E-1	–	7.9036E-1	–
12	1.8942E-1	0.99	1.7678E-1	1.47	5.3584E-1	0.95
16	1.4211E-1	0.99	1.1272E-1	1.51	4.0473E-1	0.96
24	9.4757E-2	0.99	5.8807E-2	1.60	2.7140E-1	0.98
32	7.1072E-2	0.99	3.7064E-2	1.60	2.0403E-1	0.98
$\mu=10^{-9}$						
8	2.8384E-1	–	6.8799E-2	–	7.9036E-1	–
12	1.8942E-1	0.99	4.6095E-2	0.98	5.3584E-1	0.95
16	1.4211E-1	0.99	3.4632E-2	0.99	4.0473E-1	0.96
24	9.4757E-2	0.99	2.3116E-2	0.99	2.7140E-1	0.98
32	7.1072E-2	0.99	1.7345E-2	0.99	2.0403E-1	0.98

Table 4
Example 3: Results by Taylor-Hood (Q_2,Q_1) solver on cubic meshes.

$1/h$	$\|u-u_h\|$	Rate	$\|p-p_h\|$	Rate	$\|u-u_h\|_1$	Rate
$\mu=1$						
8	6.7088E-4	–	3.6533E-3	–	4.1470E-2	–
12	1.9864E-4	3.00	1.5829E-3	2.06.	1.8445E-2	1.99
16	8.3784E-5	3.00	8.8493E-4	2.04	1.0378E-2	1.99
24	2.4821E-5	3.00	3.9193E-4	2.00	4.6133E-3	1.99
32	1.0471E-5	3.00	2.2023E-4	2.00	2.5951E-3	1.99
$\mu=10^{-9}$						
8	7.2741E+3		3.5791E-3	–	4.0657E+5	
12	1.4415E+3	Errors	1.5763E-3	2.02	1.2360E+5	Errors
16	4.5688E+2	are	8.8375E-4	2.01	5.2790E+4	are
24	9.0397E+1	too	3.9182E-4	2.00	1.5828E+4	too
32	2.8628E+1	large	2.2021E-4	2.00	6.7164E+3	large

WG Scheme II and the classical Taylor-Hood method (Q_2,Q_1) (both implemented in `deal.II`) are tested for various μ values.

As shown in Table 3, for the numerical solutions obtained from WG Scheme II, the convergence of the L^2-norms of the velocity errors is well kept at order 1, for $\mu=1$ and $\mu=10^{-9}$. The semi-norm of the discrete errors in velocity $|||\mathbf{Q}_h^\circ\mathbf{u}-\mathbf{u}_h^\circ|||$ also maintains 1st order convergence for small μ. However, as shown in Table 4, the classical Taylor-Hood solver (Q_2,Q_1) is non-robust. For $\mu=1$, all errors look good. But for $\mu=10^{-9}$, the velocity errors (in L^2- or H^1-norm) are too large.

As shown in Fig. 2, the numerical velocity component obtained from the Taylor-Hood method is spurious.

7. Concluding remarks

In this paper, we investigate numerical methods for Stokes flow by combining the weak Galerkin methodology and a lifting operator. Two finite element schemes are developed, but Scheme II based on the lifting operator is robust in the sense that the scheme maintains an optimal convergence order for errors in numerical velocity even for very small values of viscosity or large Reynolds numbers. The robustness of the novel Stokes solvers is theoretically validated (in Section 5) and numerically demonstrated (in Section 6). These solvers have been implemented in `Matlab` and `deal.II` and are readily available.

Although the paper focuses on the lowest-order cases, the approach and methodology employed here can be extended to development of robust higher order solvers. For 2-dim cases, one would readily replace $\mathrm{WG}(P_0^2,P_0^2;AC_0^2,P_0)$ by $\mathrm{WG}(P_k^2,P_k^2;AC_k^2,P_k)$ for $k\geq 1$. As for 3-dim problems, the only remaining issue is the construction of local bases for AT_k spaces for $k\geq 1$.

Data availability

Data will be made available on request.

Acknowledgements

Z. Wang was partially supported by the National Natural Science Foundation of China (grant No. 12101626) and an internal grant 74120-18841215 from Sun Yat-sen University. R. Wang was partially supported by the National Natural Science Foundation of China (grant No. 12001230, 11971198), the National Key Research and Development Program of China (grant no. 2020YFA0713602), and the Key Laboratory of Symbolic Computation and Knowledge Engineering of Ministry of Education housed at Jilin University, Changchun, 130012, P.R. China. J. Liu was partially supported by US National Science Foundation under grants DMS-1819252 and DMS-2208590.

References

[1] M. Akbas, L.G. Rebholz, Modular grad-div stabilization for the incompressible non-isothermal fluid flows, Appl. Math. Comput. 393 (2021) 125748.
[2] T. Arbogast, M.R. Correa, Two families of H(div) mixed finite elements on quadrilaterals of minimal dimension, SIAM J. Numer. Anal. 54 (6) (2016) 3332–3356.
[3] T. Arbogast, Z. Tao, Construction of H(div)-conforming mixed finite elements on cuboidal hexahedra, Numer. Math. 142 (1) (2019) 1–32.
[4] D. Arnold, D. Boffi, R. Falk, Approximation by quadrilateral finite elements, Math. Comput. 71 (2002) 909–922.
[5] D.N. Arnold, F. Brezzi, M. Fortin, A stable finite element for the Stokes equations, Calcolo 21 (4) (1984) 337–344.
[6] F. Bao, L. Mu, J. Wang, A fully computable a posteriori error estimate for the Stokes equations on polytopal meshes, SIAM J. Numer. Anal. 57 (1) (2019) 458–477.
[7] D. Boffi, F. Brezzi, M. Fortin, Mixed Finite Element Methods and Applications, Springer, 2013.
[8] C. Brennecke, A. Linke, C. Merdon, J. Schöberl, Optimal and pressure-independent L2 velocity error estimates for a modified Crouzeix-Raviart Stokes element with BDM reconstructions, J. Comput. Math. 33 (2) (2015) 191–208.
[9] F. Brezzi, R.S. Falk, Stability of higher-order Hood-Taylor methods, SIAM J. Numer. Anal. 28 (3) (1991) 581–590.
[10] L. Chen, M. Wang, L. Zhong, Convergence analysis of triangular MAC schemes for two dimensional Stokes equations, J. Sci. Comput. 63 (3) (2015) 716–744.
[11] A. Cioncolini, D. Boffi, The MINI mixed finite element for the Stokes problem: an experimental investigation, Comput. Math. Appl. 77 (2019) 2432–2446.
[12] B. Cockburn, G. Fu, W. Qiu, A note on the devising of superconvergent HDG methods for Stokes flow by M-decompositions, IMA J. Numer. Anal. 37 (2017) 730–749.
[13] B. Cockburn, G. Kanschat, D. Schötzau, A note on discontinuous Galerkin divergence-free solutions of the Navier-Stokes equations, J. Sci. Comput. 31 (1) (2007) 61–73.
[14] L.B. da Veiga, F. Brezzi, L. Marini, A. Russo, The hitchhiker's guide to the virtual element method, Math. Models Methods Appl. Sci. 24 (2014) 1541–1573.
[15] R.S. Falk, M. Neilan, Stokes complexes and the construction of stable finite elements with pointwise mass conservation, SIAM J. Numer. Anal. 51 (2) (2013) 1308–1326.
[16] A. Goharzadeh, P. Rodgers, PIV-measurements of centrifugal instabilities in a rectangular curved duct with a small aspect ratio, Fluids 6 (5) (2021).
[17] J. Guzmán, L.R. Scott, The Scott-Vogelius finite elements revisited, Math. Comput. 88 (2019) 515–529.
[18] G. Harper, J. Liu, S. Tavener, T. Wildey, Coupling Arbogast-Correa and Bernardi-Raugel elements to resolve coupled Stokes-Darcy flow problems, Comput. Methods Appl. Mech. Eng. 373 (2021) 113469.
[19] G. Harper, J. Liu, S. Tavener, B. Zheng, Lowest-order weak Galerkin finite element methods for linear elasticity on rectangular and brick meshes, J. Sci. Comput. 78 (3) (2019) 1917–1941.

[20] G. Harper, R. Wang, J. Liu, S. Tavener, R. Zhang, A locking-free solver for linear elasticity on quadrilateral and hexahedral meshes based on enrichment of Lagrangian elements, Comput. Math. Appl. 80 (2020) 1578–1595.
[21] J. Guzmán, M. Neilan, Conforming and divergence-free Stokes elements in three dimensions, IMA J. Numer. Anal. 34 (2014) 1489–1508.
[22] J. Guzmán, M. Neilan, Conforming and divergence free Stokes elements on general triangular meshes, Math. Comput. 83 (2014) 15–36.
[23] V. John, A. Linke, C. Merdon, M. Neilan, L.G. Rebholz, On the divergence constraint in mixed finite element methods for incompressible flows, SIAM Rev. 59 (3) (2017) 492–544.
[24] P.L. Lederer, Pressure Robust Discretizations for Navier-Stokes Equations: Divergence-free Reconstruction for Taylor-Hood Elements and High Order Hybrid Discontinuous Galerkin Methods, master's thesis, 2016.
[25] P.L. Lederer, A. Linke, C. Merdon, J. Schöberl, Divergence-free reconstruction operators for pressure-robust Stokes discretizations with continuous pressure finite elements, SIAM J. Numer. Anal. 55 (3) (2017) 1291–1314.
[26] P.L. Lederer, S. Rhebergen, A pressure-robust embedded discontinuous Galerkin method for the Stokes problem by reconstruction operators, SIAM J. Numer. Anal. 58 (5) (2020) 2915–2933.
[27] J. Li, X. Ye, S. Zhang, A weak Galerkin least-squares finite element method for div-curl systems, J. Comput. Phys. 363 (2018) 79–86.
[28] A. Linke, A divergence-free velocity reconstruction for incompressible flows, C. R. Acad. Sci. Paris, Ser. I 350 (2012) 837–840.
[29] A. Linke, On the role of the Helmholtz decomposition in mixed methods for incompressible flows and a new variational crime, Comput. Methods Appl. Mech. Eng. 268 (2014) 782–800.
[30] J. Liu, G. Harper, N. Malluwawadu, S. Tavener, A lowest-order weak Galerkin finite element method for Stokes flow on polygonal meshes, J. Comput. Appl. Math. 368 (2020) 112479.
[31] J. Liu, S. Tavener, Z. Wang, Lowest-order weak Galerkin finite element method for Darcy flow on convex polygonal meshes, SIAM J. Sci. Comput. 40 (5) (2018) B1229–B1252.
[32] J. Liu, S. Tavener, Z. Wang, Penalty-free any-order weak Galerkin FEMs for elliptic problems on quadrilateral meshes, J. Sci. Comput. 83 (3) (2020) 47.
[33] G. Manzini, A. Mazzia, A virtual element generalization on polygonal meshes of the Scott-Vogelius finite element method for the 2-d Stokes problem, J. Comput. Dyn. 9 (2) (2022) 207–238.
[34] K.-A. Mardal, J. Schöberl, R. Winther, A uniformly stable Fortin operator for the Taylor-Hood element, Numer. Math. 123 (3) (2013) 537–551.
[35] L. Mu, Pressure robust weak Galerkin finite element methods for Stokes problems, SIAM J. Sci. Comput. 42 (3) (2020) B608–B629.
[36] L. Mu, J. Wang, X. Ye, S. Zhang, A weak Galerkin finite element method for the Maxwell equations, J. Sci. Comput. 65 (1) (2015) 363–386.
[37] L. Mu, X. Ye, S. Zhang, Development of pressure-robust discontinuous Galerkin finite element methods for the Stokes problem, J. Sci. Comput. 89 (1) (2021) 26.
[38] M. Neda, F. Pahlevani, L.G. Rebholz, J. Waters, Sensitivity analysis of the grad-div stabilization parameter in finite element simulations of incompressible flow, J. Numer. Math. 24 (3) (2016) 189–206.
[39] N.C. Nguyen, J. Peraire, B. Cockburn, A hybridizable discontinuous Galerkin method for Stokes flow, Comput. Methods Appl. Mech. Eng. 199 (2010) 582–597.
[40] L.R. Scott, M. Vogelius, Norm estimates for a maximal right inverse of the divergence operator in spaces of piecewise polynomials, ESAIM: M2AN 19 (1) (1985) 111–143.
[41] G. Wang, L. Mu, Y. Wang, Y. He, A pressure-robust virtual element method for the Stokes problem, Comput. Methods Appl. Mech. Eng. 382 (2021) 113879.
[42] J. Wang, R. Wang, Q. Zhai, R. Zhang, A systematic study on weak Galerkin finite element methods for second order elliptic problems, J. Sci. Comput. 74 (3) (2018) 1369–1396.
[43] J. Wang, X. Ye, A weak Galerkin mixed finite element method for second-order elliptic problems, Math. Comput. 83 (2014) 2101–2126.
[44] J. Wang, Q. Zhai, R. Zhang, S. Zhang, A weak Galerkin finite element scheme for the Cahn-Hilliard equation, Math. Comput. 88 (2019) 211–235.
[45] R. Wang, X. Wang, Q. Zhai, R. Zhang, A weak Galerkin finite element scheme for solving the stationary Stokes equations, J. Comput. Appl. Math. 302 (2016) 171–185.
[46] R. Wang, R. Zhang, A weak Galerkin finite element method for the linear elasticity problem in mixed form, J. Comput. Math. 36 (2018) 469–491.
[47] H. Wei, X. Huang, A. Li, Piecewise divergence-free nonconforming virtual elements for Stokes problem in any dimensions, SIAM J. Numer. Anal. 59 (3) (2021) 1835–1856.
[48] S. Zhang, Divergence-free finite elements on tetrahedral grids for $k \geq 6$, Math. Comput. 80 (274) (2011) 669–695.
[49] L. Zhao, E.-J. Park, D.-wook Shin, A staggered DG method of minimal dimension for the Stokes equations on general meshes, Comput. Methods Appl. Mech. Eng. 345 (2019) 854–875.